Original Article

Pyrroloquinoline quinone can prevent chronic heart failure by regulating mitochondrial function

Xuan Xu[#], Chu Chen[#], Wen-Jiang Lu, Yi-Ling Su, Jia-Yu Shi, Yu-Chen Liu, Li Wang, Chen-Xi Xiao, Xiang Wu, Qi Lu

Department of Cardiology, Affiliated Hospital of Nantong University, Nantong, China

Contributions: (I) Conception and design: Q Lu, X Wu, X Xu; (II) Administrative support: Q Lu, X Wu; (III) Provision of study materials or patients: Q Lu, X Wu, X Xuan, C Chen; (IV) Collection and assembly of data: X Xu, C Chen; (V) Data analysis and interpretation: WJ Lu, YL Su, JY Shi, YC Liu, L Wang, CX Xiao; (VI) Manuscript writing: All authors; (VII) Final approval of manuscript: All authors.

[#]These authors contributed equally to this work.

Correspondence to: Qi Lu; Xiang Wu. Department of Cardiology, Affiliated Hospital of Nantong University, Nantong, China.
Email: luqint@sina.com; wuxtdfy@163.com.

Background: Myocardial mitochondrial dysfunction is the leading cause of chronic heart failure (CHF). Increased reactive oxygen species (ROS) levels, disruption of mitochondrial biogenesis and mitochondrial Ca^{2+}([Ca^{2+}]m) homeostasis and reduction of the mitochondrial membrane potential (ΔΨm) cause myocardial mitochondrial dysfunction. Therefore, treating CHF by targeting mitochondrial function is a focus of current research. For the first time, this study investigated the effects of the strong antioxidant pyrroloquinoline quinone (PQQ) on mitochondrial function in a cardiac pressure overload model, and the mechanism by which PQQ regulates [Ca^{2+}]m homeostasis was explored in depth.

Methods: After transaortic constriction (TAC), normal saline and PQQ (0.4, 2 and 10 mg/kg) were administered intragastrically to Sprague Dawley (SD) rats for 12 weeks. *In vitro*, neonatal rat left ventricle myocytes (NRVMs) were pretreated with 200 nm angiotensin II (Ang II) with or without PQQ (1, 10 and 100 μM). Rat heart remodelling was verified by assessment of atrial natriuretic peptide (ANP) and brain natriuretic peptide (BNP) levels (qRT-PCR), cell surface area (wheat germ agglutinin (WGA) staining *in vivo* and α-actin *in vitro*) and echocardiography. Myocardial mitochondrial morphology was assessed by transmission electron microscopy. Western blotting was used to assess mitochondrial biogenesis [peroxisome proliferator-activated receptor gamma coactivator 1-alpha (PGC-1α) and transcription factor A, mitochondrial (TFAM)]. The ΔΨm was determined by tetraethyl benzimidazolyl carbocyanine iodide (JC-1) staining and flow cytometry, and ROS levels were measured by dichloro-dihydro-fluorescein diacetate (DCFH-DA) and MitoSOX Red staining. [Ca^{2+}]m was measured by isolating rat mitochondria, and mitochondrial Ca^{2+} channel proteins [the mitochondrial Na^{+}/Ca^{2+} exchanger (NCLX) and mitochondrial Ca^{2+} uniporter (MCU)] were detected by Western blot.

Results: *In vivo* and *in vitro*, PQQ pretreatment improved pressure overload-induced cardiac remodelling and cell hypertrophy, thus preventing the occurrence of CHF. PQQ also prevented mitochondrial morphology damage and reduced the PGC-1α and TFAM downregulation caused by TAC or Ang II. In addition, in NRVMs treated with Ang II+PQQ, PQQ regulated ROS levels and increased the ΔΨm. PQQ also regulated [Ca^{2+}]m homeostasis and prohibited [Ca^{2+}]m overloading by increasing NCLX expression.

Conclusions: These results show that PQQ can prevent [Ca^{2+}]m overload by increasing NCLX expression and thereby reducing ROS production and protecting the ΔΨm. At the same time, PQQ can increase PGC-1α and TFAM expression to regulate mitochondrial biogenesis. These factors can prevent mitochondrial dysfunction, thereby reducing cardiac damage caused by pressure overload and preventing the occurrence of CHF.

Keywords: Chronic heart failure (CHF); pyrroloquinoline quinone (PQQ); mitochondrial dysfunction; [Ca^{2+}]m overload

Submitted Jan 27, 2019. Accepted for publication Apr 01, 2020.
doi: 10.21037/cdt-20-129
View this article at: http://dx.doi.org/10.21037/cdt-20-129

Introduction

Chronic heart failure (CHF) is usually caused by systolic or diastolic dysfunction (1). Mitochondria, as important organelles for maintaining heart function, provide energy for each heartbeat (2). Increasing evidence suggests that mitochondria are the power plant of the heart; however, like an old battery, the heart will eventually be depleted in patients with CHF (3). Mitochondrial dysfunction and the development of CHF, especially heart failure caused by pressure overload, are causal and vicious cycles (4). The pathological mechanisms of mitochondrial disorders are very complex and include mitochondrial Ca^{2+} ($[Ca^{2+}]m$) homeostasis, protein modification regulation, mitochondrial membrane potential ($\Delta\Psi m$), and mitochondrial redox. In cases of CHF, mitochondrial biogenesis changes, redox imbalances, $[Ca^{2+}]m$ homeostasis alterations, and increased mitochondrial permeability transition pore (mPTP) openings occur (3,5). Therefore, the prevention of mitochondrial dysfunction has become an effective treatment for CHF (6).

Pyrroloquinoline quinone (PQQ) is a known potent antioxidant cofactor that is widely distributed in animal and plant tissues and is an indispensable nutrient in mammals (7), as PQQ deprivation affects mitochondria and mitochondrial function in these species (8). In an insulinoma cell line (INS-1), PQQ can reduce reactive oxygen species (ROS) levels and improve apoptosis (9). In contrast, in human chondrosarcoma cells, PQQ can increase ROS levels and promote tumour cell apoptosis (10). However, regardless of the decreases and increases in ROS levels, PQQ protects tissues by regulating the redox reaction. Moreover, PQQ protects the function of the corresponding tissue by improving the mitochondrial function of the liver, neurons and other tissues (8,11). It can also reduce autophagy and atrophy in mouse skeletal muscles (12). However, the role of PQQ in CHF caused by pressure overload is unknown.

In normal myocardial cells, mitochondrial Ca^{2+} uniporter (MCU) is responsible for $[Ca^{2+}]m$ uptake, and the mitochondrial Na^{+}/Ca^{2+} exchanger (NCLX) is responsible for $[Ca^{2+}]m$ discharge balance the $[Ca^{2+}]m$ content (13,14). However, previous studies have shown that in heart failure, $[Ca^{2+}]m$ overload occurs because this balance is disrupted, and NCLX overexpression reduces $[Ca^{2+}]m$ accumulation and protects heart function (14). These results prove the importance of $[Ca^{2+}]m$ in the treatment of heart failure. In the present study, we aimed to investigate the mitochondrial mechanisms through which PQQ is involved in Ang II-induced neonatal rat left ventricle myocytes (NRVMs) model and in a transaortic constriction (TAC) surgery-induced cardiac pressure overload Sprague Dawley (SD) rat model. We evaluated the effects of PQQ on NRVM mitochondrial biogenesis, mitochondrial morphology, $\Delta\Psi m$, ROS, and mitochondrial $[Ca^{2+}]m$ to explore a new treatment for CHF.

Methods

Animal model

Six-week-old SD rats (190–220 g, male) were anaesthetized with an intraperitoneal injection of 10% chloral hydrate (3 $mL \cdot kg^{-1}$) and then subjected to TAC (15) (n=42); or sham surgery (n=20). On the second day after surgery, 30 rats were selected randomly for intragastric PQQ treatment with high, medium and low doses (0.4, 2, 10 mg/kg). PQQ was purchased from Nascent Health Sciences LLC (New York, USA) in its disodium salt form (PureQQ®). All other rats were intragastrically administered 2 mL of saline. All rats were maintained under the same temperature, humidity, and light conditions and had free access to food. Twelve weeks after the operation, echocardiography (VisualSonics, Canada) was used to validate the development of CHF. After echocardiography, the rats were sacrificed, and their hearts were isolated and stored in liquid nitrogen. All animal procedures were approved by the Ethics Committee of Nantong University, and all studies were performed in accordance with the Guide for the Care and Use of Laboratory Animals (US National Institutes of Health; revised 1996).

NRVM culture and treatment

Hearts were isolated from 2-day-old SD rats and rinsed 3 times with phosphate buffered saline (PBS) on ice. The LVs from the rats were fully pulverized to a mud-like

consistency. Digestion was performed with collagenase II (1 mg/mL; 1148090 Sigma-Aldrich, USA) at 37 ℃ for 8 minutes, and the supernatants were centrifuged at 120 rpm for 5 minutes to obtain a pellet. The digested heart fragments were collected, and the above steps were repeated 8–10 times. NRVMs were cultured in Dulbecco's modified Eagle's medium (DMEM; Gibco, USA) containing 10% foetal bovine serum. After 48 h of incubation, some NRVMs were pretreated with 1, 10 and 100 μM PQQ for 24 h. After pretreatment, 200 nm Ang II was added to the NRVMs with or without PQQ treatment for 48 h to establish an *in vitro* model of cardiac pressure overload.

Isolation of mitochondria

Rats were euthanized, and their hearts were placed on ice. The LV was cut into small pieces on ice, resuspended and homogenized in 3 mL of buffer (1× protease inhibitor mixture, 500 mM sucrose, 20 mM Tris, 2 mM EDTA, pH 7.4). Then, the samples were centrifuged at 1,000 ×g for 10 minutes, and the supernatants were removed. Next, the supernatants were centrifuged at 10,000 ×g for 20 minutes at 4 ℃. The mitochondrial pellets were collected and used within 1 hour. Specific experimental protocols were performed in accordance with previously published standard procedures (16). According to the manufacturer's instructions, a $[Ca^{2+}]$m assay kit (#701220, Cayman Chemical, USA) was used to determine the $[Ca^{2+}]$m content in rat hearts within one hour.

Mitochondrial membrane potential assays

To assay NRVM ΔΨm, NRVMs were collected and resuspended in cell culture medium. Then, 0.5 mL of JC-1 dye working solution (C2006, Beyotime, China) was added at 37 ℃ for 20 minutes. Then, the samples were centrifuged at 600 ×g for 4 minutes at 4 ℃, and the supernatants were discarded. Next, 1 mL of JC-1 dye buffer (1×) was added to resuspend the cells, which were centrifuged at 600 ×g for 4 minutes at 4 ℃, and the supernatants were discarded. This procedure was repeated three times. The cells were then subjected to flow cytometry analysis.

To assay the ΔΨm in rat myocardial tissue, rat hearts frozen in liquid nitrogen were sectioned at a thickness of 10 μm, and a frozen section ΔΨm staining kit (JC-1 method, GMS10013.4, Genmed Scientific Inc., USA) was utilized. First, the dye and dilution solutions were mixed at a ratio of 1:100 to obtain a working solution, and 500 μL of a rinsing solution was then added to the section and incubated at room temperature for 10 minutes. Next, the sections were covered with 200 μL of the working solution and incubated at 37 ℃ for 20 minutes. Finally, 500 μL of the rinse solution was added for 10 minutes. After rinsing, the slides were mounted and observed under a confocal scanning microscope (BX41, Olympus, Japan).

NRVM surface area measurement

NRVMs were fixed with 4% paraformaldehyde at room temperature for 20 minutes, and 0.5% Triton X-100 was applied for 20 minutes to increase the permeability of the NRVM membrane. Next, the membranes were blocked with bovine serum albumin (BSA) for 1.5 h and incubated with a primary antibody against α-actin (1:150; A7811 Sigma-Aldrich, USA) overnight at 4 ℃. The membranes were then incubated with the appropriate secondary antibodies for 1.5 h at room temperature. Finally, the nuclei were stained blue with 6-dimidyl-2-phenylindole dihydrochloride (DAPI; C1005 Beyotime, China), and the NRVMs were observed using a confocal scanning microscope (BX41, Olympus, Japan).

ROS assays

The cell culture fluid was removed from NRVMs, and DCFH-DA (1:1,000; S0033 Beyotime, China) was added at 10 μM for 20 minutes at 37 ℃. Then, the cells were washed three times with cell culture solution and viewed under a confocal scanning microscope (488 nm excitation wavelength, 525 nm emission wavelength; BX41, Olympus, Japan). Mitochondrial ROS levels were measured by staining with MitoSOX Red (M36008 Thermo Fisher Scientific, USA). After treatment with or without PQQ or Ang II, MitoSOX Red was added to the NRVMs and incubated for 30 minutes at 37 ℃. Subsequently, the NRVMs were washed three times, and the mitochondrial ROS level was observed using a confocal scanning microscope (BX41, Olympus, Japan). SOD1/2 activity was detected by a kit according to the manufacturer's instructions (s0103 Beyotime, China).

Transmission electron microscopy

Heart mitochondria were observed by transmission electron microscopy according to a previously described protocol. Briefly, LV samples were placed in 2.5% glutaraldehyde

and fixed in 1% osmium tetroxide. Then, the sections were cut into small pieces and observed under a transmission electron microscope (JEOL, JEM-1230, Japan).

Western blot analysis

NRVMs and rat LVs were collected and lysed, and total protein was separated on SDS-polyacrylamide gels and transferred to PVDF membranes. The PVDF membranes were then blocked with 5% skim milk powder for 1.5 h and incubated with the following primary antibodies overnight: PGC-1α (1:1,000; ABE868 Sigma, USA), TFAM (1:1,000; ABS2083 Sigma, USA), NCLX (1:1,000; PA5-50827 Invitrogen, USA), MCU (1:1,000; HPA016480 Sigma, USA), SOD1 (1:1,000; SAB1406464 Sigma, USA), SOD2 (1:1,000; SAB2102261 Sigma, USA), collagen I (1:1,000; ab34710 Abcam, USA), collagen III (1:1,000; ab184993 Abcam, USA), GAPDH (1:1,000; ab181602 Abcam, USA), VDAC1 (1:1,000; ab15895 Abcam, USA) and tubulin (1:1,000; T3526 Sigma, USA). Then, the membranes were incubated with specific horseradish peroxidase-conjugated secondary antibodies at 37 ℃ for 1.5 h, and Quantity One software (Bio-Rad, USA) was used to quantify the Western blot bands.

Histological analysis

Rat heart tissues were cryosectioned. To detect cardiomyocyte size and myocardial fibrosis, the cryosections were subjected to wheat germ agglutinin (WGA; 1 mg/mL; L9640 Sigma-Aldrich, USA) and Masson's triple staining. The images were quantitatively analysed by fluorescence microscopy (BX41, Olympus, Japan) using Image-Pro Plus (IPP) 6.0 software.

Quantitative RT-PCR analysis

Total RNA was extracted from NRVMs and LV tissues by TRIzol reagent (Invitrogen, USA). According to the manufacturer's instructions, a RevertAid First Strand cDNA Synthesis Kit (Thermo Scientific, USA) was used to reverse transcribe the RNA into cDNA, and LightCycler® 480 SYBR Green I Master Mix (Roche) was used to quantify the relative mRNA expression. The mRNA analysis and amplification conditions were the same. The primer sequences used in this study were as follows: rat ANP F: 5'-ATGGGCTCCTTCTCCATCAC-3', R: 5'-TTTCTCCTCCAAGGTGGTC-3'; rat BNP F: 5'-AGTCTCCAGAACAATCCACGATGC-3', R: 5'-CCGGAAGGCGCTGTCTTGAG-3'; rat GAPDH F: 5'-GGCACAGTCAAGGCTGAGAATG-3', R: 5'-ATGGTGGTGAAGACGCCAGTA-3'.

The relative levels were determined by the $2^{-\Delta\Delta Ct}$ method, and the experiment was repeated 3 times independently.

Statistical analysis

All statistical tests were performed with GraphPad Prism 6.0 software. All data are presented as the mean ± standard deviation. T tests and analysis of variance (ANOVA) were used for comparisons between two groups and among multiple groups, respectively, and $P<0.05$ indicated statistical significance.

Results

PQQ improves CHF and dysfunction caused by pressure overload

To determine the effect of PQQ on CHF and systolic function *in vivo*, SD rats were subjected to sham or TAC surgery for 12 weeks and administered a daily dose of 0.4, 2 or 10 mg/kg PQQ. After 12 weeks of TAC, SD rats showed significant ventricular and myocyte hypertrophy, as evidenced by increased heart sizes (*Figure 1A*) and increased heart weight/body weight (HW/BW) ratios (*Figure 1B*). These changes were attenuated by PQQ (2 and 10 mg/kg) in TAC rats compared to sham rats. Echocardiography assessments showed that TAC-induced left ventricular contractile function (*Figure 1C*), as indicated by a decreased ejection fraction (EF)% (*Figure 1D*) and fractional shortening (FS)% (*Figure 1E*), was reversed by PQQ (0.4, 2 and 10 mg/kg BW). The left end-systolic internal diameter was also higher in the TAC group than in the sham group (*Figure 1F*). The 2 and 10 mg/kg PQQ doses significantly reduced these unfavourable alterations. Interestingly, compared with the control conditions, PQQ treatment at 0.4 mg/kg increased the FS% (*Figure 1E*), while the left ventricular diameter was smaller (*Figure 1F*). The 2 and 10 mg/kg PQQ doses also had greater effects on the mRNA expression levels of heart failure markers [atrial natriuretic peptide (ANP) and brain natriuretic peptide (BNP)] than the control (*Figure 1G,H*). The above findings indicated that 2 and 10 mg/kg PQQ treatment had good therapeutic effects; however, compared with 2 mg/kg PQQ, 10 mg/kg PQQ showed no concentration-dependent effect, and 2 mg/kg PQQ was thus the best therapeutic dose among the

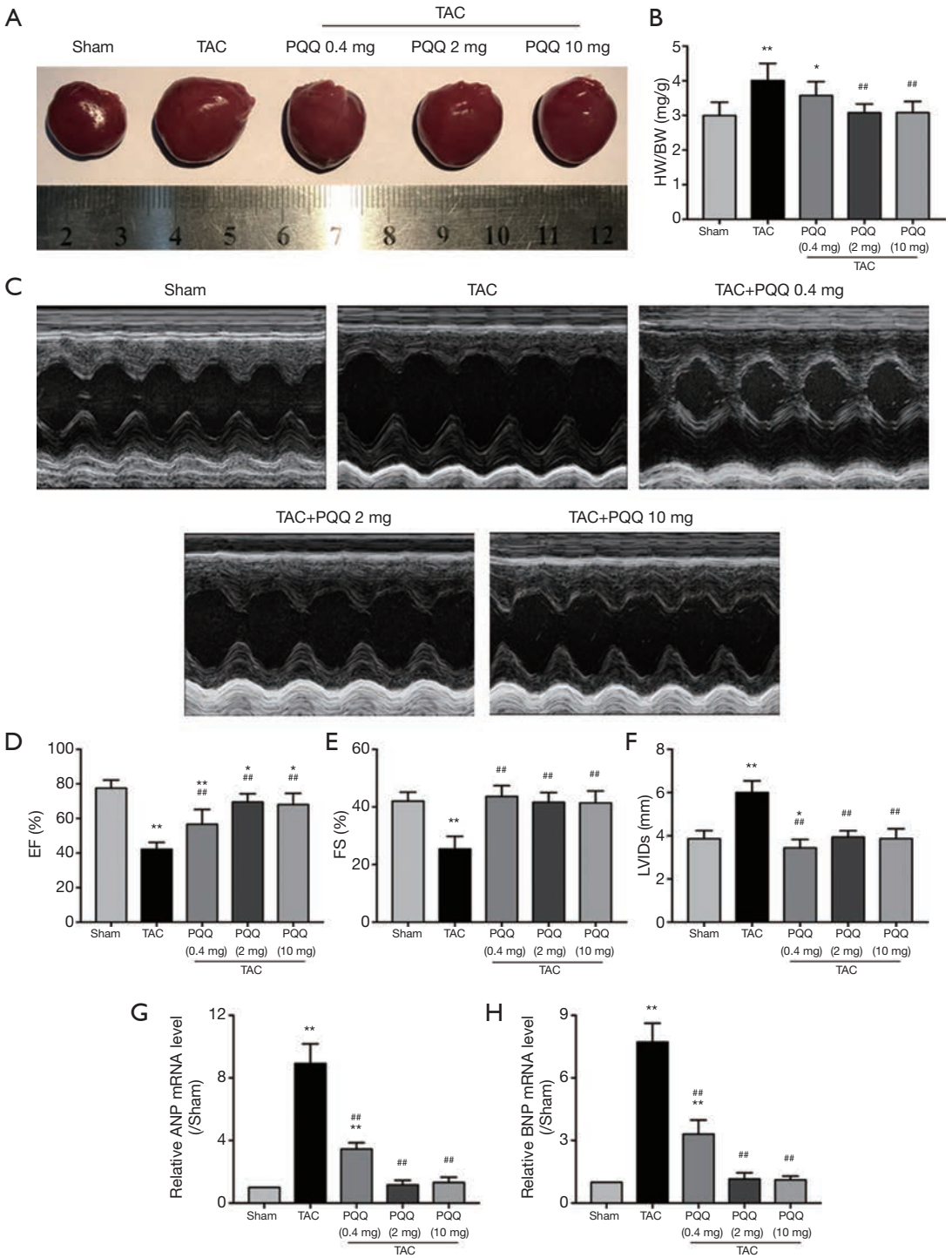

Figure 1 PQQ could delay or prohibit CHF development. The optimal dose of PQQ for intragastric administration to rats was determined. (A) Heart sizes of rats treated with or without PQQ (0.4, 2 and 10 mg/kg) administered intragastrically 12 weeks after TAC or sham surgery. (B) Ratio of heart weight and body weight (HW/BW). (C) M-mode echocardiographic images of the left ventricle along the left parasternal long axis. (D,E,F) Heart failure parameters as determined by echocardiography (left ventricular ejection fraction, left ventricular fraction shortening and left ventricular internal diameter at end-systole). (G,H) Real-time PCR quantitative analysis of heart failure markers (ANF and BNP) in rat left ventricular tissue. The data are expressed as the mean ± SD. *P<0.05; **P<0.01 *vs.* sham. $^{\#}$P<0.05; $^{\#\#}$P<0.01 *vs.* TAC. PQQ, pyrroloquinoline quinone; CHF, chronic heart failure; TAC, transaortic constriction; ANF, atrial natriuretic peptide; BNP, brain natriuretic peptide.

three groups. In the following experiments, 2 mg/kg PQQ was administered to the TAC+PQQ treatment group. As ventricular myocyte enlargement and fibrosis are hallmarks of cardiac hypertrophic remodelling, we examined the effect of PQQ on the left ventricle (LV) cardiomyocyte size (*Figure 2B,D*) and collagen deposition (*Figure 2A,C*). We also verified the expression of the fibrosis-related protein collagen I/III (*Figure 2E,F,G*). After 12 weeks of TAC, the SD rats showed increased cardiomyocyte areas, collagen deposition and mRNA expression levels of heart failure markers (ANP and BNP); these effects were markedly reduced in the PQQ+TAC group.

In vitro, we treated NRVMs with 200 nM angiotensin II (Ang II) for 48 h to simulate a cardiac pressure overload model and measured the surface area of NRVMs (*Figure 3A*). Pretreatment with 10 and 100 μM PQQ reversed the changes in ANP and BNP mRNA expression (*Figure 3B,C*) and the surface area of NRVMs (*Figure 3D*). There was no significant difference between 10 and 100 μM PQQ pretreatment. Therefore, in subsequent experiments, the Ang II + PQQ group was pretreated with 10 μM PQQ. Taken together, these results indicate that PQQ improves CHF and heart dysfunction.

Relationship of PQQ with mitochondrial morphology

Rat LV heart tissue was observed under a transmission electron microscope, and the results indicated that the mitochondrial morphology became increasingly severe after TAC (*Figure 4A*). Compared with the healthy group, the TAC-treated group exhibited blurred mitochondrial cristae, reduced mitochondrial areas (*Figure 4B,C*), mitochondrial swelling (*Figure 4D*) and disorganized sarcomere and mitochondrial arrangements (*Figure 4A*). PQQ treatment after TAC protected the morphology of mitochondria in the rat heart, as the mitochondrial morphological changes described above were not observed in the TAC + PQQ group. As shown in the figure, early PQQ treatment prevented morphological changes in the heart mitochondria caused by cardiac pressure overload and helped maintain heart mitochondrial function.

Prevention of mitochondrial deterioration by PQQ

Because mitochondrial biogenesis is also critical for mitochondrial function, we investigated the effects of PQQ on mitochondrial biogenesis in rat hearts and NRVMs by Western blotting to quantitatively assess the protein levels of peroxisome proliferator-activated receptor gamma coactivator 1alpha (PGC-1α) and transcription factor A, mitochondrial (TFAM) (*Figure 5A*). As expected, PGC-1α (*Figure 5B*) and TFAM (*Figure 5C*) expression was decreased in TAC-damaged cardiac mitochondria, and the early use of PQQ delayed this phenomenon. We also observed the same phenomenon *in vitro* (*Figure 5D*). The PGC-1α and TFAM expression in Ang II-induced NRVMs was also downregulated, which was prevented by pretreatment with PQQ (*Figure 5E,F*). Based on the above data, we further verified that PQQ could protect heart mitochondrial function by preventing mitochondrial biogenesis changes *in vivo* and *in vitro*.

PQQ reduces ROS levels and delays mitochondrial membrane potential (ΔΨm) decline

Mitochondrial redox not only provides the heart with large amounts of adenosine triphosphate (ATP) but also produces ROS. Importantly, excessive ROS in cells can have pathological effects. Thus, we used a dichlorodihydrofluorescein diacetate (DCFH-DA) probe to measure ROS levels in NRVMs (*Figure 6A*), with the green fluorescence intensity indicating the ROS level, and PQQ pretreatment attenuated the increase in Ang II-induced ROS levels. In addition, we used a MitoSOX Red probe to measure mitochondrial ROS levels in NRVMs (*Figure 6B*), with the red fluorescence intensity indicating the mitochondrial ROS levels, and PQQ pretreatment attenuated the increase in Ang II-induced mitochondrial ROS levels. In addition, we examined superoxide dismutase 1 (SOD1) and superoxide dismutase 2 (SOD2) protein expression (*Figure 6C,D,E*) by Western blot, revealing no difference in SOD1 expression among the groups, SOD2 expression was increased by PQQ treatment. We also tested SOD1 and SOD2 activity (*Figure 6F,G*), and the surface activity of SOD2 in the TAC + PQQ group was significantly greater than that in the TAC group.

ROS imbalance, in turn, decreases the ΔΨm (16,17). We hypothesized that PQQ could delay ΔΨm depolarization, and we assessed the ΔΨm in the LV and NRVMs by tetraethyl benzimidazolyl carbocyanine iodide (JC-1) staining. The results validated our hypothesis that the early use of PQQ reduced the JC-1 monomer amount in the interventricular septum as determined by the corresponding reduction in green fluorescence intensity. The JC-1 aggregate was converted to the JC-1 monomer after TAC in rat heart mitochondria (*Figure 7A*). *In vitro*, we performed

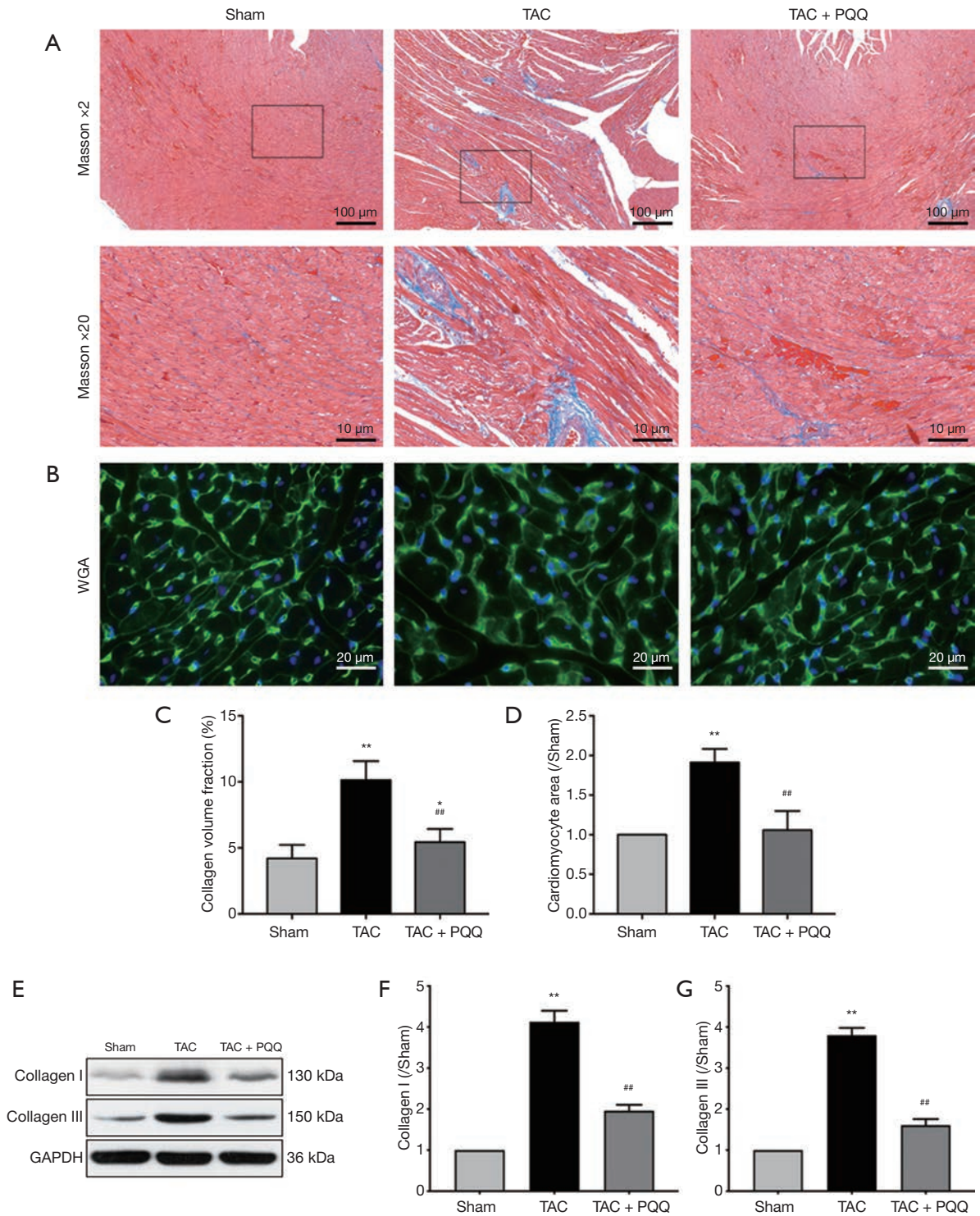

Figure 2 PQQ inhibited pathological myocardial remodelling in rats at 12 weeks after TAC. (A) Representative images of Masson's triple-stained LV tissue sections; scale bars: 100 and 10 μm. (B) WGA staining of rat LV tissue cardiomyocyte cross-sections; scale bars: 20 μm. (C) Quantitative analysis of fibrosis. (D) Quantification of cardiomyocyte size in cardiomyocyte cross-sections. (E) Western blotting analyses of collagen I and collagen III in the sham, TAC, and TAC+PQQ groups. (F,G) Quantification of the collagen I and collagen III protein levels in rat LV tissue. The data are expressed as the mean ± SD. *P<0.05; **P<0.01 *vs.* sham. $^{\#}$P<0.05; $^{\#\#}$P<0.01 *vs.* TAC. PQQ, pyrroloquinoline quinone; TAC, transaortic constriction.

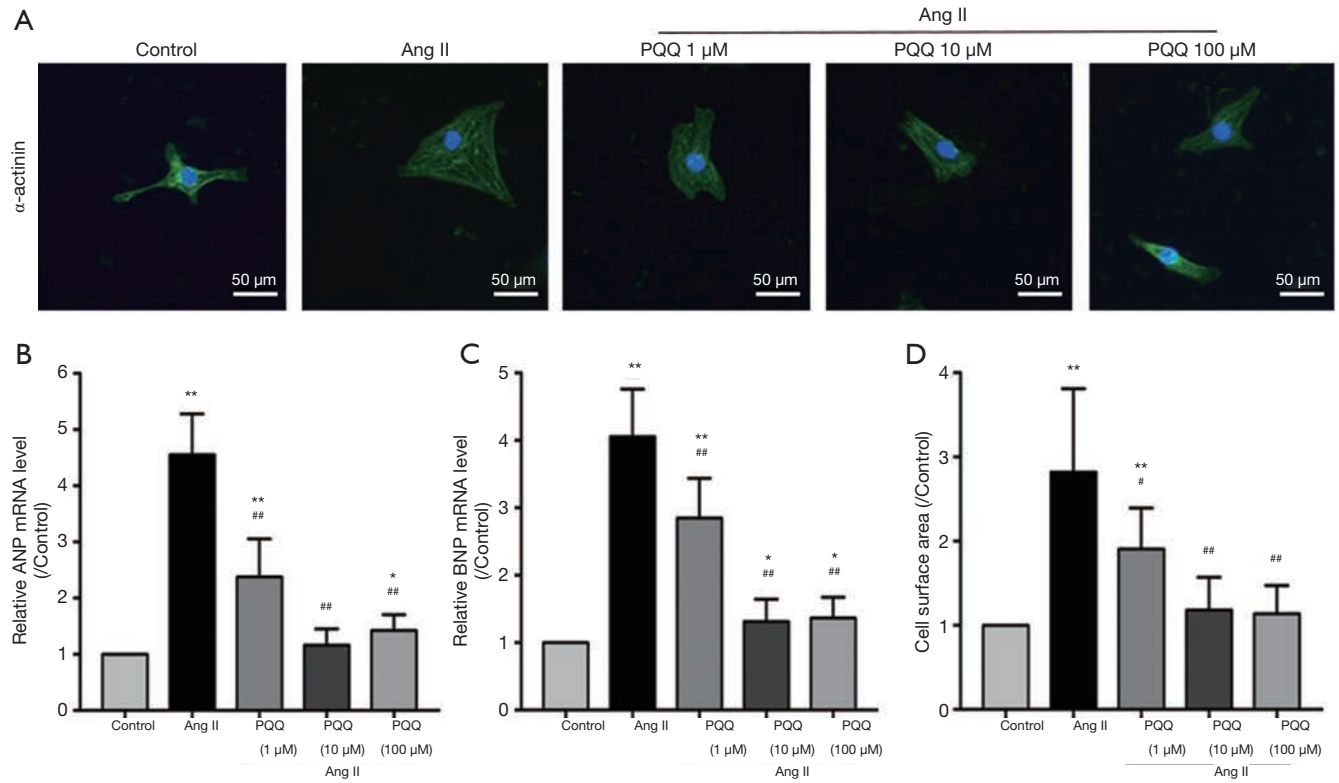

Figure 3 PQQ inhibited NRVM hypertrophy induced by Ang II (200 nm; 48 h). The optimal dose of PQQ *in vitro* was determined. (A) α-Actinin staining of NRVMs in the presence of Ang II (200 nm for 48 h) after treatment with PQQ (1, 10 and 100 μM). The nucleus and cytoskeleton are labelled with DAPI (blue) and α-actinin (green). Scale bar: 50 μm. (B) Quantitative analysis of the NRVM cell areas in the above groups. (C,D) Real-time PCR quantitative analysis of heart failure markers (ANP and BNP) in NRVMs. The data are expressed as the mean ± SD. *P<0.05; **P<0.01 *vs.* control. #P<0.05; ##P<0.01 *vs.* Ang II. PQQ, pyrroloquinoline quinone; NRVMs, neonatal rat left ventricle myocytes; DAPI, 6-dimidyl-2-phenylindole dihydrochloride; ANF, atrial natriuretic peptide; BNP, brain natriuretic peptide.

ΔΨm bivariate JC-1 analysis of NRVMs using flow cytometry. Ang II-induced NRVMs showed a decreased ΔΨm, and PQQ pretreatment prevented Ang II-induced ΔΨm depolarization (*Figure 7B*). Overall, both *in vivo* and *in vitro*, PQQ reduced ROS levels in damaged cells while also maintaining ΔΨm levels, thereby protecting mitochondrial function.

Mitochondrial Ca^{2+} ($[Ca^{2+}]m$) overload is suppressed by PQQ

Mitochondrial Ca^{2+} uptake and uncoordinated efflux cause $[Ca^{2+}]m$ overload, which is accompanied by a decrease in the ΔΨm and an increase in ROS levels (3). However, the increase in SOD2 activity does not fully explain the restoration of ROS levels. Therefore, analysis of $[Ca^{2+}]m$ indicates not only the effects of PQQ but also the cause of the abovementioned events. To measure $[Ca^{2+}]m$ in rats, we isolated rat myocardial mitochondria and used an o-cresolphthalein complexone assay to determine the $[Ca^{2+}]m$ content. As shown in *Figure 8A*, the $[Ca^{2+}]m$ overload caused by TAC was relieved by PQQ pretreatment. Next, we measured the expression of MCU and NCLX in the rat myocardium to investigate how PQQ protects $[Ca^{2+}]m$ homeostasis (*Figure 8B*). The Western blot results showed no differences in MCU expression among the three groups (*Figure 8C*), but PQQ pretreatment reversed the decrease in NCLX induced by cardiac pressure overload (*Figure 8D*). The protective effects on NCLX explained how early PQQ treatment regulated $[Ca^{2+}]m$ homeostasis, and PQQ treatment promoted $[Ca^{2+}]m$ efflux and prohibited $[Ca^{2+}]m$ overload. The phenomena observed in NRVMs were the same as those observed in the rat myocardium (*Figure 8E,F,G*). In summary, PQQ pretreatment protected the expression of NCLX but had no effect on MCU.

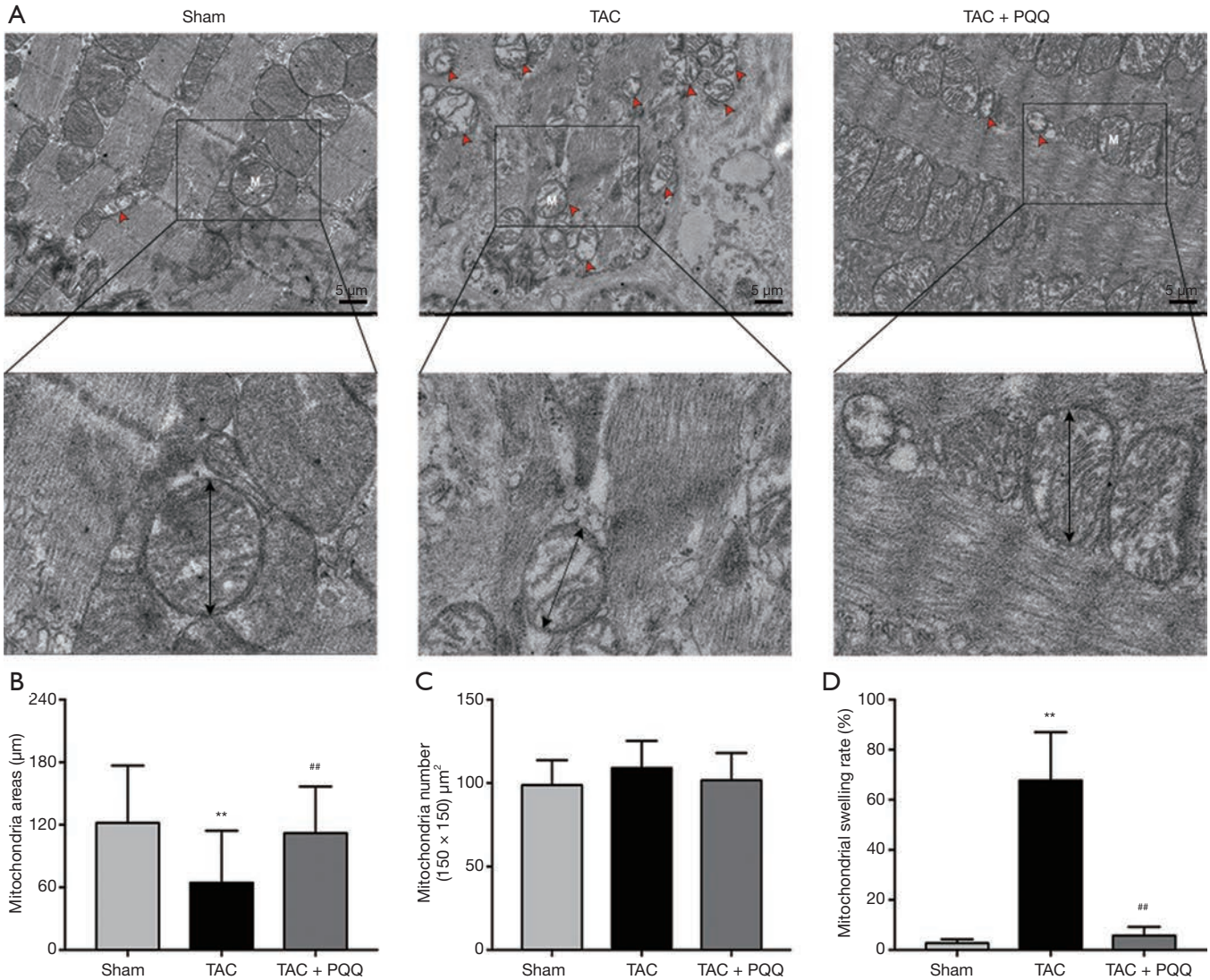

Figure 4 PQQ treatment did not significantly alter the morphology of mitochondria in rat LV tissue at 12 weeks after TAC. (A) Representative images of LV tissue from the sham, TAC, and TAC+PQQ groups acquired by transmission electron microscopy. The red arrow represents blurred mitochondrial cristae and mitochondrial swelling. Magnification: 5,000×. An enlarged view of the representative mitochondria is shown in the following figure. (B) Quantification of mitochondrial size in LV tissues. (C) The number of mitochondria within the same surface area. (D) Swelling rate of mitochondria in the same number of mitochondria. The data are expressed as the mean ± SD. *P<0.05; **P<0.01 *vs.* sham. $^{\#}$P<0.05; $^{\#\#}$P<0.01 *vs.* TAC. PQQ, pyrroloquinoline quinone; TAC, transaortic constriction.

Discussion

CHF is, to some extent, caused by a mismatch between high energy consumption and low energy supply, and this difference in supply and demand cycles viciously in the heart (18,19). Mitochondria, as the "power house", provide the heart with most of its ATP, and targeting mitochondria has gradually become a foundation of CHF treatment (20). Therefore, the research and development of drugs that target mitochondrial function have also become popular (21).

$[Ca^{2+}]$ m is very active and acts as a second messenger to regulate mitochondrial function (22,23). In fact, $[Ca^{2+}]$ m overload increases heart mitochondrial ROS and reactive nitrogen species (RNS) production (24), and excessive Ca^{2+} accumulation in mitochondria causes ΔΨm depolarization, opens mPTP, and releases cyt-c to activate the mitochondria-

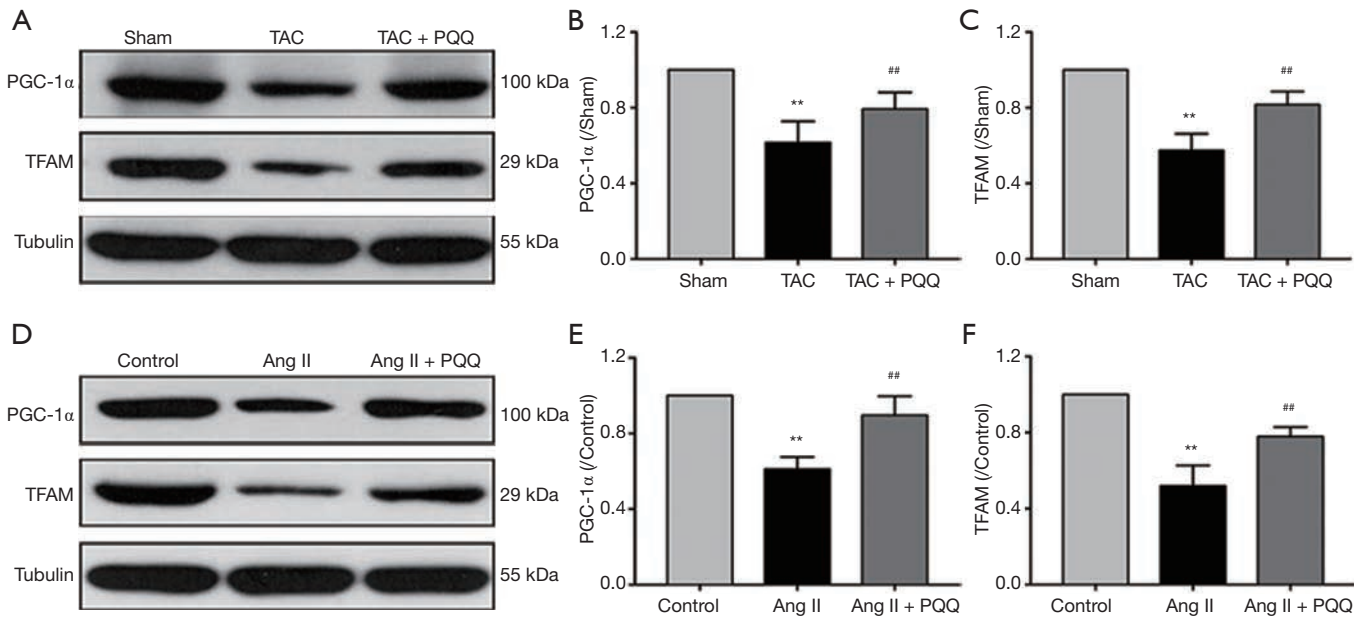

Figure 5 PQQ reduced mitochondrial biogenesis dysfunction caused by pressure overload both *in vivo* and *in vitro*. (A) Western blot analyses of PGC-1α and TFAM in the sham, TAC, and TAC+PQQ groups. (B,C) Quantification of the PGC-1α and TFAM protein levels in rat LV tissue. The data are expressed as the mean ± SD. *P<0.05; **P<0.01 *vs.* sham. #P<0.05; ##P<0.01 *vs.* TAC; (D) Western blot analyses of PGC-1α and TFAM in the control, Ang II, and Ang II+PQQ groups. (E,F) Quantification of the PGC-1α and TFAM protein levels in NRVMs. The data are expressed as the mean ± SD. *P<0.05; **P<0.01 *vs.* control. #P<0.05; ##P<0.01 *vs.* Ang II.

dependent death pathway (25). ROS imbalance decreases the ΔΨm, which fosters the production of ROS, constituting another vicious cycle (16), and the early prevention and treatment of mitochondrial dysfunction are therefore very important. NCLX was found to be responsible for mitochondrial $[Ca^{2+}]$m efflux into the cytoplasm (26). In NCLX-deficient mice produced by crossing $Slc8b1^{fl/fl}$ mice with αMHC-MerCreMer mice, $[Ca^{2+}]$m overload triggered heart failure (14). In mice overexpressing NCLX, $[Ca^{2+}]$m overload did not occur after myocardial infarction (MI), indicating better myocardial remodelling (14). These studies reinforce the role of NCLX in heart mitochondria. Another protein, MCU, mainly functions to translocate Ca^{2+} from the cytoplasm into mitochondria (13), and conditional MCU knockout in mice was shown to prevent $[Ca^{2+}]$m overload and decrease hypoxic/ischaemic (HI) brain injury (27). Compared to normal mice with heart failure, $Mcu^{-/-}$ mouse models did not show abnormalities upon TAC- or isoprotemol-induced cardiac pressure overload (28). Moreover, in our experiments, neither rats with cardiac pressure overload induced by TAC or Ang II-induced NRVMs showed changes in MCU expression. PQQ treatment protected NCLX expression, reduced $[Ca^{2+}]$m overload and prevented CHF.

PQQ is a strong antioxidant, and early research has shown that it can penetrate mitochondria (29). Various studies have further elucidated the mechanism by which PQQ clears ROS. In renal tubular epithelial cells, PQQ can increase the levels of SOD2 and catalase (CAT), thereby clearing ROS (30). In mouse brain endothelial cells under high-glucose conditions, PQQ reduces ROS production by inhibiting the c-Jun N-terminal kinase (JNK) pathway (31). Furthermore, in H9C2 cells subjected to oxygen/glucose deprivation, PQQ inhibits the activation of the phosphoinositide 3-kinase (PI3K)/AKT pathway, thereby preventing the production of excess ROS (32). In our study, we explored whether PQQ could reduce ROS production in a cardiac pressure overload model by preventing $[Ca^{2+}]$m overload. In the heart, ROS play a physiological role at appropriate levels, but an abnormal increase in ROS production can have pathological effects (33,34). Increased ROS levels damage mitochondrial biogenesis and cause mitochondrial dysfunction (35). During CHF development, mitochondrial dysfunction and abnormal increases in ROS levels are reciprocal events. Our experiments showed that PQQ could ameliorate ROS production to appropriate

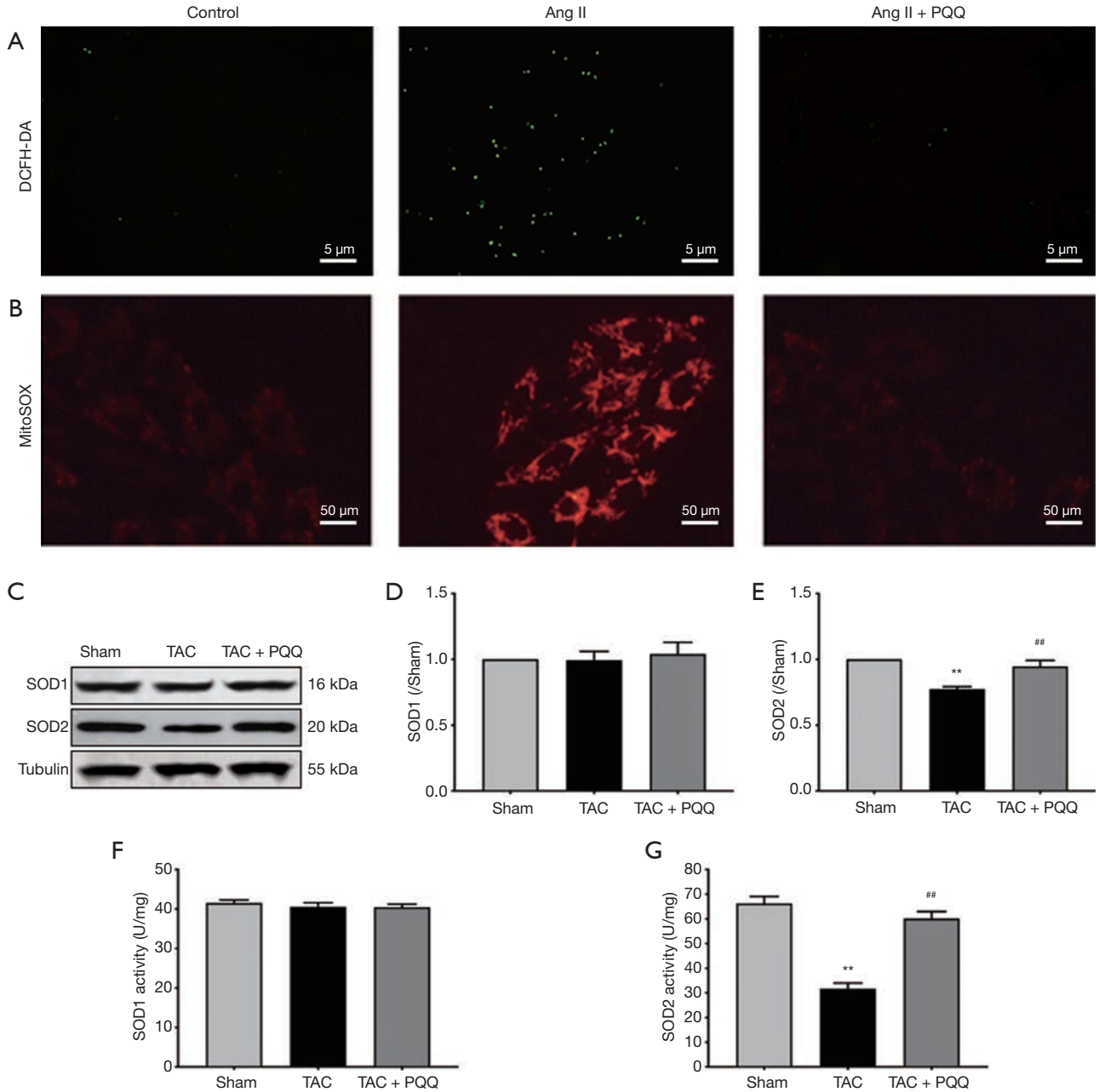

Figure 6 PQQ prevented abnormal increases in ROS levels in Ang II-induced NRVMs. (A) ROS levels were determined using DCFH-DA staining after treatment with PQQ and Ang II in NRVMs. Scale bars: 5 μm. (B) Mitochondrial ROS levels in NRVMs after treatment with PQQ and Ang II were determined by MitoSOX Red staining. Scale bars: 50 μm. (C) Western blot analyses of SOD1 and SOD2 in the Shame, TAC, and TAC+PQQ groups. (D,E) Quantification of the SOD1 and SOD2 protein expression in rat LV tissue. (F,G) SOD1 and SOD2 activity in the above groups. The data are expressed as the mean ± SD. *P<0.05; **P<0.01 *vs.* Sham. #P<0.05; ##P<0.01 *vs.* TAC.

levels, thus prohibiting imbalance.

Electron leakage from electron transport chain (ETC) complexes I and III (CI, CIII) results in the release of superoxide into the mitochondrial matrix and membrane space (36), which at least partially explains why the mitochondrial morphology is disrupted. Previously, PQQ

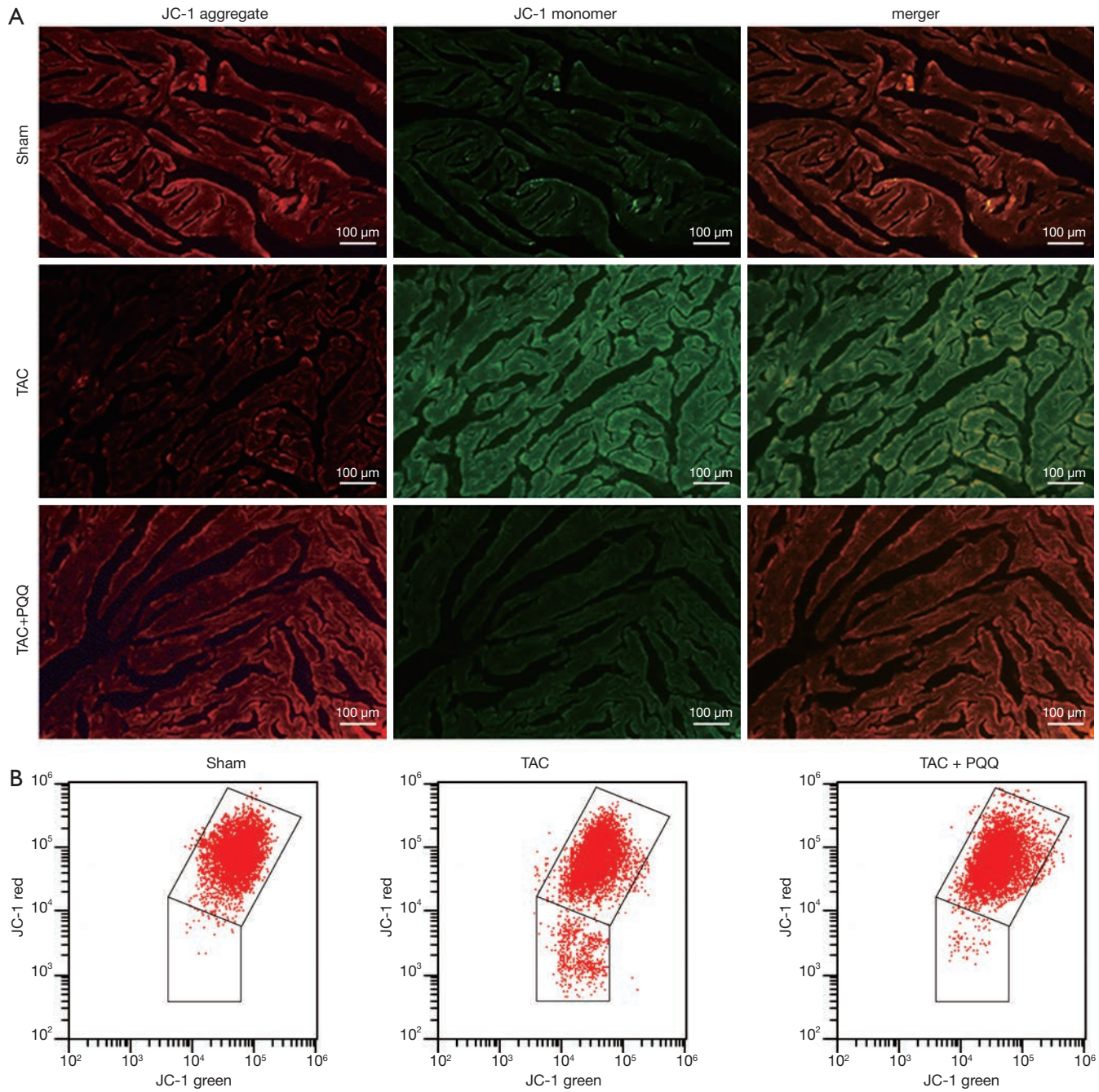

Figure 7 PQQ prevented a decrease in the ΔΨm *in vivo* and *in vitro*. (A) The LV tissue mitochondrial membrane potential was determined by staining with the mitochondrial dye JC-1. Red fluorescence represents JC-1 aggregates in healthy cells with a high mitochondrial membrane potential, whereas green fluorescence highlights JC-1 monomers in cells with a low ΔΨm. Scale bar =100 μm. (B) In NRVMs, ΔΨm was assayed by flow cytometry using JC-1 staining.

treatment was shown to protect the function of ETC complexes in skeletal muscle mitochondria (37). The above data demonstrate that PQQ may maintain mitochondrial morphology by protecting ETC complex function, which is potentially related to the mechanism via which PQQ protects the heart.

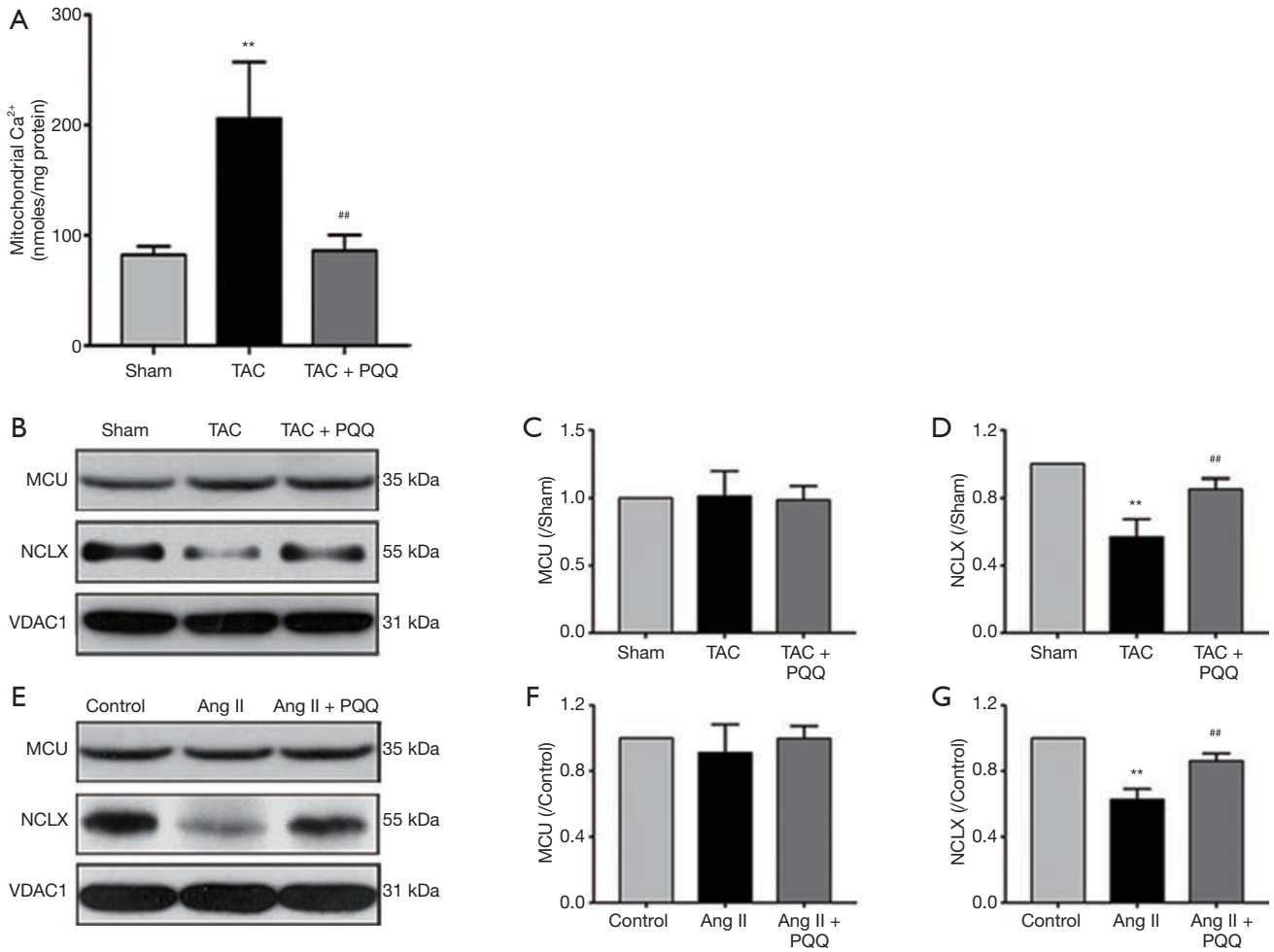

Figure 8 PQQ improved $[Ca^{2+}]m$ homeostasis and reduced $[Ca^{2+}]m$ overload by maintaining NCLX levels. (A) The o-cresolphthalein complexone assay was used to determine the Ca^{2+} content in purified mitochondria isolated from rat myocardia. (B) Western blot analyses of MCU and NCLX in the sham, TAC, and TAC+PQQ groups. (C,D) Quantification of the MCU and NCLX protein levels in rat LV tissue. The data are expressed as the mean ± SD. *P<0.05; **P<0.01 *vs.* sham. $^{\#}$P<0.05; $^{\#\#}$P<0.01 *vs.* TAC. (E) Western blot analyses of MCU and NCLX in the control, Ang II, and Ang II+PQQ groups. (F, G) Quantification of the MCU and NCLX protein levels in NRVMs. The data are expressed as the mean ± SD. *P<0.05; **P<0.01 *vs.* control. $^{\#}$P<0.05; $^{\#\#}$P<0.01 *vs.* Ang II.

Previous experiments confirmed that PQQ can activate the NAD-dependent deacetylase sirtuin-1 (SIRT1)/PGC-1α signalling pathway in mouse National Institutes of Health (NIH)/3T3 fibroblasts to promote mitochondrial biogenesis (38). In the cardiac pressure overload model, the absence of PGC-1α is likely to cause HF (39). After TAC, pathological remodelling of the heart can be reduced by the maintenance of PGC-1α expression (40), and the expression of TFAM and nuclear factor erythroid-1/2-related factor (Nrf1/2) was shown to be promoted by PGC-1α (41). Our experiments demonstrated that PQQ could also prevent the formation of CHF by maintaining PGC-1α expression in rat hearts and NRVMs, and we also verified that PQQ treatment did not decrease TFAM expression. Furthermore, $[Ca^{2+}]m$ overload was observed in a mouse model of TFAM deficiency (42), proving that PQQ may improve $[Ca^{2+}]m$ overload via this mechanism. We first demonstrated that PQQ could improve mitochondrial biogenesis in cardiac pressure overload models both *in vitro* and *in vivo*. These findings are also consistent with the improvements in mitochondrial biogenesis in other models treated with PQQ.

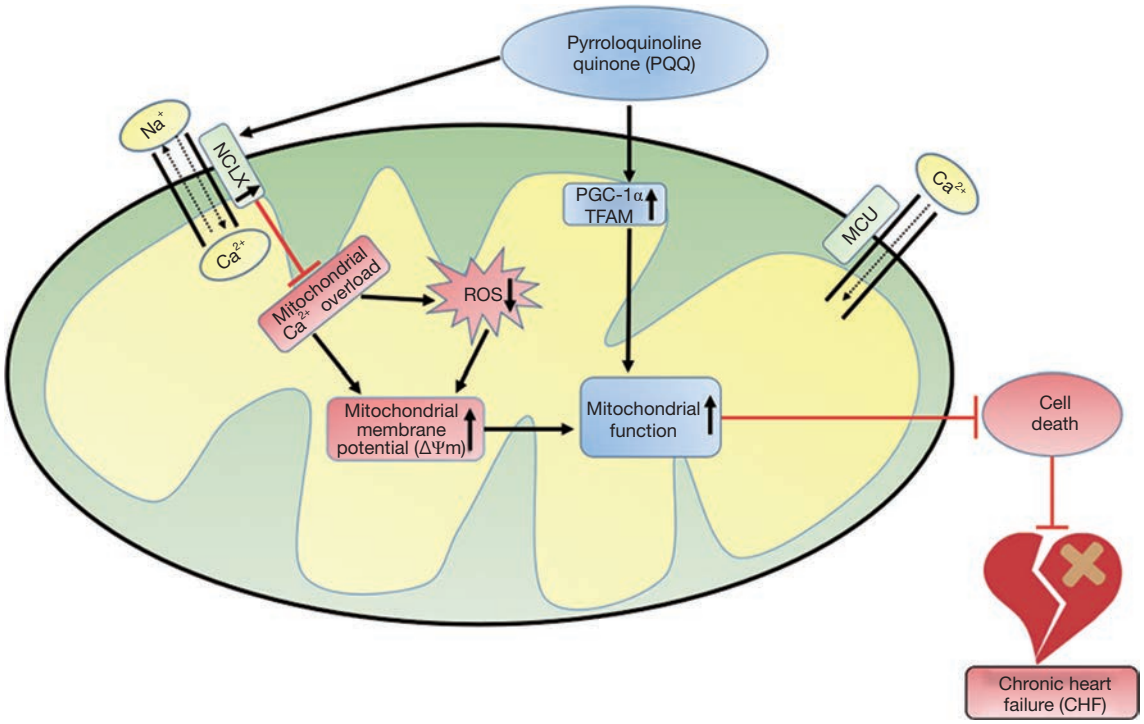

Figure 9 Schematic diagram: PQQ can prevent $[Ca^{2+}]m$ overload by increasing NCLX expression and thereby reducing ROS production and increasing the ΔΨm. At the same time, PQQ can increase PGC-1α and TFAM expression to regulate mitochondrial biogenesis. These factors can prevent mitochondrial dysfunction, thereby reducing cardiac damage caused by pressure overload and preventing the occurrence of CHF.

Herein, PQQ could alleviate the decrease in the ΔΨm and the production of ROS in TAC-treated rat hearts and Ang II-induced NRVMs, suggesting that it regulates $[Ca^{2+}]m$ homeostasis. This hypothesis was verified by measuring the Ca^{2+} content in rat heart mitochondria, and the effect of PQQ on NCLX expression was determined. It was concluded that PQQ may reduce ROS production and maintain the ΔΨm by regulating $[Ca^{2+}]m$ homeostasis through NCLX. However, $[Ca^{2+}]m$ homeostasis in mitochondria is very complicated, and the specific impact of PQQ on $[Ca^{2+}]m$ efflux and uptake and whether PQQ affects cytosolic Ca^{2+} and sarcoplasmic reticulum Ca^{2+} needs to be further verified. The specific mechanism by which PQQ increases NCLX also needs to be further clarified. Previous studies have shown that in cardiomyocytes lacking TFAM, NCLX transcript levels decrease as TFAM expression decreases, which promotes mitochondrial calcium overload (42), similar to the results observed herein. The decreased and increased expression levels of NCLX and TFAM may be correlated. Moreover, decreased expression of the frataxin (FXN) gene also increases NCLX expression in mitochondria (43). PQQ can be utilized in mitochondrial therapy, but its potential effects on FXN need to be further investigated. NCLX is a member of the Na^+/Ca^{2+} exchanger (NCX) family, and NCX proteins are cleaved by some calpains (44), which may also be related to NCLX expression. Related experiments will be performed in our next study.

Conclusions

In summary, we verified for the first time that PQQ can regulate $[Ca^{2+}]m$ homeostasis by increasing NCLX expression, thereby reducing ROS production and preventing a decrease in the ΔΨm. In addition, we demonstrated that PQQ can upregulate PGC-1α and TFAM to improve mitochondrial biogenesis and maintain mitochondrial morphology. These results verified that PQQ can prevent mitochondrial dysfunction induced by cardiac pressure overload and slow or prevent the

development of CHF.

Acknowledgments

Funding: This work was supported by the Nantong Science and Technology Bureau, China (grant nos. JC2018082 and MS22018005).

Footnote

Conflicts of Interest: All authors have completed the ICMJE uniform disclosure form (available at http://dx.doi.org/10.21037/cdt-20-129). The authors have no conflict of interests to declare.

Ethical Statement: The authors are accountable for all aspects of the work in ensuring that questions related to the accuracy or integrity of any part of the work are appropriately investigated and resolved. All animal procedures in this study were carried out in accordance with the recommendations of the Institutional Animal Care and Use Committee of Nantong University, and were approved by the Institutional Animal Care and Use Committee of Nantong University (No. 20170305-003).

References

1. Ramani GV, Uber PA, Mehra MR. Chronic Heart Failure: Contemporary Diagnosis and Management. Mayo Clin Proc 2010;85:180-95.
2. Kumar AA, Kelly DP, Chirinos JA. Mitochondrial Dysfunction in Heart Failure With Preserved Ejection Fraction. Circulation 2019;139:1435-50.
3. Zhou B, Tian R. Mitochondrial dysfunction in pathophysiology of heart failure. J Clin Invest 2018;128:3716-26.
4. Chaanine AH, Joyce LD, Stulak JM, et al. Mitochondrial Morphology, Dynamics, and Function in Human Pressure Overload or Ischemic Heart Disease With Preserved or Reduced Ejection Fraction. Circ Heart Fail 2019;12:e005131.
5. Ribeiro Junior RF, Dabkowski ER, Shekar KC, et al. MitoQ improves mitochondrial dysfunction in heart failure induced by pressure overload. Free Radic Biol Med 2018;117:18-29.
6. Murphy MP, Hartley RC. Mitochondria as a therapeutic target for common pathologies. Nat Rev Drug Discov 2018;17:865-86.
7. Akagawa M, Nakano M, Ikemoto K. Recent progress in studies on the health benefits of pyrroloquinoline quinone. Biosci Biotechnol Biochem 2016;80:13-22.
8. Chowanadisai W, Bauerly KA, Tchaparian E, et al. Pyrroloquinoline Quinone Stimulates Mitochondrial Biogenesis through cAMP Response Element-binding Protein Phosphorylation and Increased PGC-1α Expression. J Biol Chem 2010;285:142-52.
9. Shi L, Jiang L, Zhang X, et al. Pyrroloquinoline quinone protected autophagy-dependent apoptosis induced by mono(2-ethylhexyl) phthalate in INS-1 cells. Hum Exp Toxicol 2020;39:194-211.
10. Wen L, Lu X, Wang R, et al. Pyrroloquinoline quinone induces chondrosarcoma cell apoptosis by increasing intracellular reactive oxygen species. Mol Med Rep 2018;17:7184-90.
11. Lu J, Chen S, Shen M, et al. Mitochondrial regulation by pyrroloquinoline quinone prevents rotenone-induced neurotoxicity in Parkinson's disease models. Neurosci Lett 2018;687:104-10.
12. Ma W, Zhang R, Huang Z, et al. PQQ ameliorates skeletal muscle atrophy, mitophagy and fiber type transition induced by denervation via inhibition of the inflammatory signaling pathways. Ann Transl Med 2019;7:440.
13. Baughman JM, Perocchi F, Girgis HS, et al. Integrative genomics identifies MCU as an essential component of the mitochondrial calcium uniporter. Nature 2011;476:341-5.
14. Luongo TS, Lambert JP, Gross P, et al. The mitochondrial Na+/Ca2+ exchanger is essential for Ca2+ homeostasis and viability. Nature 2017;545:93-7.
15. Nakamura Y, Kita S, Tanaka Y, et al. A disintegrin and metalloproteinase 12 prevents heart failure by regulating cardiac hypertrophy and fibrosis. Am J Physiol Heart Circ Physiol 2020;318:H238-51.
16. Santulli G, Xie W, Reiken SR, et al. Mitochondrial calcium overload is a key determinant in heart failure. Proc Natl Acad Sci U S A 2015;112:11389-94.
17. Rizwan H, Pal S, Sabnam S, et al. High glucose augments

ROS generation regulates mitochondrial dysfunction and apoptosis via stress signalling cascades in keratinocytes. Life Sci 2020;241:117148.
18. Ozcan C, Li Z, Kim G, et al. Molecular Mechanism of the Association Between Atrial Fibrillation and Heart Failure Includes Energy Metabolic Dysregulation Due to Mitochondrial Dysfunction. J Card Fail 2019;25:911-20.
19. Smith CS, Bottomley PA, Schulman SP, et al. Altered creatine kinase adenosine triphosphate kinetics in failing hypertrophied human myocardium. Circulation 2006;114:1151-8.
20. Brown DA, Perry JB, Allen ME, et al. Expert consensus document: Mitochondrial function as a therapeutic target in heart failure. Nat Rev Cardiol 2017;14:238-50.
21. Siasos G, Tsigkou V, Kosmopoulos M, et al. Mitochondria and cardiovascular diseases-from pathophysiology to treatment. Ann Transl Med 2018;6:256.
22. Kerkhofs M, Bultynck G, Vervliet T, et al. Therapeutic implications of novel peptides targeting ER-mitochondria Ca-flux systems. Drug Discov Today 2019;24:1092-103.
23. Hopper RK, Carroll S, Aponte AM, et al. Mitochondrial matrix phosphoproteome: effect of extra mitochondrial calcium. Biochemistry 2006;45:2524-36.
24. Yeh CH, Shen ZQ, Hsiung SY, et al. Cisd2 is essential to delaying cardiac aging and to maintaining heart functions. PLoS Biol 2019;17:e3000508.
25. Zhu H, Jin Q, Li Y, et al. Melatonin protected cardiac microvascular endothelial cells against oxidative stress injury via suppression of IP3R-[Ca]c/VDAC-[Ca]m axis by activation of MAPK/ERK signaling pathway. Cell Stress Chaperones 2018;23:101-13.
26. Iwaki M, Refaeli B, van Dijk L, et al. Structure-affinity insights into the Na and Ca interactions with multiple sites of a sodium-calcium exchanger. FEBS J 2020;febs.15250.
27. Nichols M, Pavlov EV, Robertson GS. Tamoxifen-induced knockdown of the mitochondrial calcium uniporter in Thy1-expressing neurons protects mice from hypoxic/ischemic brain injury. Cell Death Dis 2018;9:606.
28. Holmström KM, Pan X, Liu JC, Menazza S, Liu J, Nguyen TT, et al. Assessment of cardiac function in mice lacking the mitochondrial calcium uniporter. J Mol Cell Cardiol. 2015;85:178-82.
29. Stites T, Storms D, Bauerly K, et al. Pyrroloquinoline quinone modulates mitochondrial quantity and function in mice. J Nutr 2006;136:390-6.
30. Wang Z, Li Y, Wang Y, et al. Pyrroloquinoline quinine protects HK-2 cells against high glucose-induced oxidative stress and apoptosis through Sirt3 and PI3K/Akt/FoxO3a signaling pathway. Biochem Biophys Res Commun 2019;508:398-404.
31. Wang Z, Chen GQ, Yu GP, et al. Pyrroloquinoline quinone protects mouse brain endothelial cells from high glucose-induced damage in vitro. Acta Pharmacol Sin 2014;35:1402-10.
32. Xu F, Yu H, Liu J, et al. Pyrroloquinoline quinone inhibits oxygen/glucose deprivation-induced apoptosis by activating the PI3K/AKT pathway in cardiomyocytes. Mol Cell Biochem 2014;386:107-15.
33. Song M, Chen Y, Gong G, et al. Super-suppression of mitochondrial reactive oxygen species signaling impairs compensatory autophagy in primary mitophagic cardiomyopathy. Circ Res 2014;115:348-53.
34. Hamanaka RB, Chandel NS. Mitochondrial reactive oxygen species regulate cellular signaling and dictate biological outcomes. Trends Biochem Sci 2010;35:505-13.
35. Peoples JN, Saraf A, Ghazal N, et al. Mitochondrial dysfunction and oxidative stress in heart disease. Exp Mol Med 2019;51:1-13.
36. Wong HS, Dighe PA, Mezera V, et al. Production of superoxide and hydrogen peroxide from specific mitochondrial sites under different bioenergetic conditions. J Biol Chem 2017;292:16804-9.
37. Kuo YT, Shih PH, Kao SH, et al. Pyrroloquinoline Quinone Resists Denervation-Induced Skeletal Muscle Atrophy by Activating PGC-1α and Integrating Mitochondrial Electron Transport Chain Complexes. PLoS One 2015;10:e0143600.
38. Saihara K, Kamikubo R, Ikemoto K, et al. Pyrroloquinoline Quinone, a Redox-Active o-Quinone, Stimulates Mitochondrial Biogenesis by Activating the SIRT1/PGC-1alpha Signaling Pathway. Biochemistry 2017;56:6615-25.
39. Lv J, Deng C, Jiang S, et al. Blossoming 20: The Energetic Regulator's Birthday Unveils its Versatility in Cardiac Diseases. Theranostics 2019;9:466-76.
40. Piquereau J, Moulin M, Zurlo G, et al. Cobalamin and folate protect mitochondrial and contractile functions in a murine model of cardiac pressure overload. J Mol Cell Cardiol 2017;102:34-44.
41. Vega RB, Kelly DP. Cardiac nuclear receptors: architects of mitochondrial structure and function. J Clin Invest 2017;127:1155-64.
42. Sommakia S, Houlihan PR, Deane SS, et al. Mitochondrial cardiomyopathies feature increased uptake and diminished efflux of mitochondrial calcium. J Mol Cell Cardiol 2017;113:22-32.

43. Purroy R, Britti E, Delaspre F, et al. Mitochondrial pore opening and loss of Ca exchanger NCLX levels occur after frataxin depletion. Biochim Biophys Acta Mol Basis Dis 2018;1864:618-31.

44. Wanichawan P, Hafver TL, Hodne K, et al. Molecular basis of calpain cleavage and inactivation of the sodium-calcium exchanger 1 in heart failure. J Biol Chem 2014;289:33984-98.

Cite this article as: Xu X, Chen C, Lu WJ, Su YL, Shi JY, Liu YC, Wang L, Xiao CX, Wu X, Lu Q. Pyrroloquinoline quinone can prevent chronic heart failure by regulating mitochondrial function. Cardiovasc Diagn Ther 2020. doi: 10.21037/cdt-20-129